



Friction and wear behavior of sintered magnesium composite reinforced with CNT-Mg₂Si/MgO

Junko Umeda, Katsuyoshi Kondoh*, Hisashi Imai

Joining and Welding Research Institute, Osaka University, 11-1, Mihogaoka, Ibaragi, Osaka 567-0047 Japan

ARTICLE INFO

Article history:

Received 28 August 2008

Received in revised form 18 October 2008

Accepted 27 October 2008

Keywords:

Magnesium

SiO₂

Mg₂Si

Carbon nanotube

Friction coefficient

Powder metallurgy

ABSTRACT

In order to improve and evaluate the wear behavior of the sintered magnesium materials under dry sliding conditions, the effect of carbon nanotubes (CNTs) and Mg₂Si/MgO compounds, which were reinforcements of the sintered material, on the friction coefficient and wear loss under dry conditions was discussed. One of the raw materials was amorphous and porous silica particles originated from rice husks, which were coated with CNTs and contained nanotubes in the pores. The in situ synthesis of Mg₂Si and MgO via deoxidization and oxidation reaction occurred from the elemental mixture of pure magnesium and CNT-SiO₂ composite particles via the spark plasma sintering process. The friction coefficient of the composite material was low and stable because of no adhesion and stick-slip phenomenon in contacting with the SUS304 stainless steel ball as a counter material. The wear rate of sintered magnesium materials decreases in increasing the content of CNTs and Mg₂Si. The friction coefficient was proportional to the total wear loss of magnesium materials. These results were due to both of the defensive by hard Mg₂Si dispersoids and self-lubricant effect by network nanotubes on the sliding surface.

© 2008 Elsevier B.V. All rights reserved.

1. Introduction

Recently magnesium alloys are widely applied to structural components both to reduce the energy consumption and to improve the mobility of personal digital assistants because they are lightest of the industrial metals in the practical use. They are, however, poor to the mechanical properties, such as Young's modulus, tensile strength, hardness and heat resistance. In particular, when applying them to friction materials, the wear or seizure phenomena easily occur by contacting with the counter materials [1–3]. Therefore, the additives of hard particles and lubricants are effective to improve the mechanical and tribological properties of the conventional magnesium alloys [4–7]. On the other hand, carbon nanotubes (CNTs), showing excellent characteristics such as high tensile strength, high elastic modulus, and high hardness, have been considered as useful and attractive additives to organic materials [8,9], bulky metals [10,11] and metallic coatings [12,13] for tribological and structural applications. In particular, according to the theoretical consideration [14], a friction coefficient between the walls of multi-walled CNTs should be extremely low. That is, CNT has a significant self-lubricant property by nano-ball bearing effects [15]. The bundles of CNTs are easily formed during

the conventional mixing or blending under dry conditions due to van der Waals forces at the most-surface carbon atoms between CNTs. Unfortunately, they cause the decrease of mechanical and wear properties because their bundles have poor bonding to the matrix. In order to obtain a stable and low friction coefficient, it is important to control the nanotubes left out from the matrix of the composites during contacting with the counterparts in sliding. On the other hand, magnesium silicides (Mg₂Si) intermetallics are one of the effective dispersoids to improve the mechanical and tribological performance of magnesium alloys because of their high hardness of 350–700 Hv [16]. They are easily synthesized by the solid-state reaction of magnesium powder and silicon or silica particles with exothermic heat [17]. By the synthesis of Mg₂Si compounds from the elemental mixture of Mg and SiO₂ powders, the magnesium composites reinforced with Mg₂Si/MgO particles show a good wear resistance and anti-offensive performance in sliding wear test under oil lubricant [18]. In this study, CNT-SiO₂ composite particles have been employed as the reinforcements of the sintered magnesium materials to obstruct the CNTs dropped out from their matrix in sliding. Porous structured SiO₂ particles, originated from rice husks [19], were used as raw materials, and dipped into the solutions including un-bundled CNTs. The composite powders were elementally mixed with the magnesium powder, and sintered after cold compaction. The microstructural analysis and evaluation of the mechanical and tribological behavior of the sintered magnesium reinforced with CNTs and Mg₂Si/MgO com-

* Corresponding author. Fax: +81 6 6879 4369.

E-mail address: kondoh@jwri.osaka-u.ac.jp (K. Kondoh).

pounds. The effects of Mg₂Si hard particles and nanotubes on the friction coefficient, surface damages and wear loss of the sintered magnesium material were investigated by using the ball on disc wear test equipment under dry conditions.

2. Experimental

2.1. Rice husk silica particles

In order to prepare amorphous silica particles with a purity of 99% or more from rice husks, the citric acid (C₆H₈O₇) leaching treatment was applied to them at 323 K for 1.8 ks for the removal of metallic impurities such as Ca, K, Na, via chelate reaction [20]. After water rinsing and air drying at 373 K of the rice husks, they were combusted at 1073 K for 3.6 ks under an air supplement of 2.5 ml/s to control the crystallization of original amorphous silica during burning [21]. The fragmentation and refinement of the rice husk ashes were carried out by using a ball milling equipment (SEIWA GIKEN, RM-05) for 900 s under a dry condition. Their particle size was measured by Laser Diffraction Particle Size Analyzer (HORIBA, Partica LA-920), and their morphology was observed by field-emission scanning electron microscope (FE-SEM, JOEL, JSM-6500F) with energy dispersive X-ray spectrometer (EDX). The mean particle size and specific surface area of them were 12.6 μm and 187 m²/g, respectively.

2.2. CNT-SiO₂ composite particles

Multi-wall carbon nanotubes (MWCNTs, Bayer Material Science), having a diameter of about 10 nm and 1–3 μm length, were used as raw materials. Another raw materials were refined porous silica particles with a large specific surface area of 180–200 m²/g [22]. They were dipped into the surfactant solution dispersed with un-bundled nanotubes to prepare the CNT-SiO₂ composite particles. With regard to the solutions dispersed with completely split nanotubes, polar zwitterions generally had a high solubility in water, but a poor solubility in most organic solvents [23]. 3-(N,N-dimethylstearylammonio) propanesulfonate, a typical linear zwitterionic surfactant, was used in this study. It had both hydrophobic and hydrophilic groups. Electrostatic interactions, having larger attractive forces than the van der Waals forces between CNTs, occurred at the hydrophilic because of the positive and negative charges on their headgroups. As a result, the un-bundled CNTs were dispersed in the zwitterionic surfactant solution [23]. By dipping the silica particles into the solution, their surface was covered with the un-bundled CNTs due to the negative zeta potential of silica particles with –61.8 mV (pH 8.28) in the solution kept at 298 K. The CNTs also entered the continuous pores of the silica, and existed inside the particles. After air drying at 353 K of the porous silica particles, SEM observation was carried out to clarify that the CNTs uniformly existed not only on the surface, but also inside the pores of the silica particles.

2.3. Preparation of sintered magnesium reinforced with CNT-SiO₂ composite particles

The elemental mixture of the above CNT-SiO₂ composite particles and pure magnesium powders, having a mean particle size of 182 μm and 98.8% purity, were prepared as the starting materials. They were filled into the steel die with a diameter of 45 mm, and consolidated at room temperature by using a 2000 kN hydraulic press machine. Their green compacts with a relative density of 77–79% were sintered at 823 K by spark plasma sintering (SPS, Syntex Inc., SPS-1030) under 30 MPa pressure in vacuum to synthesize Mg₂Si intermetallics via a solid-state reaction. The sintered

magnesium composite material including CNT-Mg₂Si/MgO reinforcements was used as a disk specimen of wear test.

2.4. Evaluation

SEM observation on amorphous and porous silica particles coated with CNTs was carried out. Differential thermal analysis (DTA, Shimadzu, DTG-60) was taken place on the silica particles and the elemental mixture of silica and pure magnesium powders from 295 K to 973 K under an argon gas supplement with 2.5 ml/s to evaluate the reaction behavior of the silica coated with CNTs and the elementally mixed powders. XRD and SEM-EDS analysis were used to detect the in situ formed intermetallics of the magnesium composites during sintering. Rock-well type hardness (F-scale, 1.59 mm diameter steel ball was used) of the sintered material was measured by using a hardness testing machine (Mitutoyo, ARK-600). The density of each sintered magnesium material was measured by the Archimedes method. The wear behavior of the P/M sintered magnesium composite reinforced with the CNT-Mg₂Si was investigated by using a ball on disk wear test equipment (RHESCA CO LTD., FPR-2100) under an air condition. A SUS304 stainless steel ball with 1.9 mm diameter was used as the counter material. The sliding speed was 55 mm/s, and applied load from the SUS304 ball was controlled at 0.5 N. The friction radius and sliding distance of this wear test were 3 mm and 33 m, respectively. A change in the friction coefficient was automatically calculated from the measured friction torque between the SUS304 ball and the sintered magnesium disk specimen by PC.

3. Results and discussion

3.1. Reactivity and microstructures

Fig. 1 shows an amorphous silica powder, which contains nanotubes in the intra-pores. It consists of the primary ultra-fine silica particles less than 1–2 μm. The primary silica reveals a spherical shape, not angular, because they were fractured during a long time ball milling process under a low energy density in milling. The added CNTs are completely de-bundled, and dispersed on the silica particles as shown by the arrows. Fig. 2 indicates DTA profiles of the CNT-SiO₂ composite particles and the elemental mixture of magnesium powders with the composite particles (CNT-SiO₂ content; 10 mass%) in heating up to 973 K. No exothermic and endothermic heat is detected in the profile of the CNT-SiO₂ composite particles. That is, no reaction between nanotubes and amorphous silica particles occurs, and silicon carbides (SiCs) are not formed in heating less than the melting point of pure magnesium (923 K). In the case of the elemental mixture of magnesium powders with CNT-SiO₂ composite particles, the exothermic is observed at 720 K, and the exothermic reaction with an extremely large heat occurs at 776 K. The previous study showed the sintering temperature at 765 K or more was enough to synthesize Mg₂Si intermetallics from the elemental mixture of magnesium and SiO₂ powders by both deoxidization and oxidation reactions in a solid state [18]. From a thermodynamic point of view as shown in the below, this reaction reasonably occurs.



Therefore, when heating the CNT-SiO₂ composite particles, the ignition temperature accompanying a large exothermic heat shown in Fig. 2 corresponds to the starting temperature to synthesize both Mg₂Si and MgO via the deoxidization and oxidation reaction.

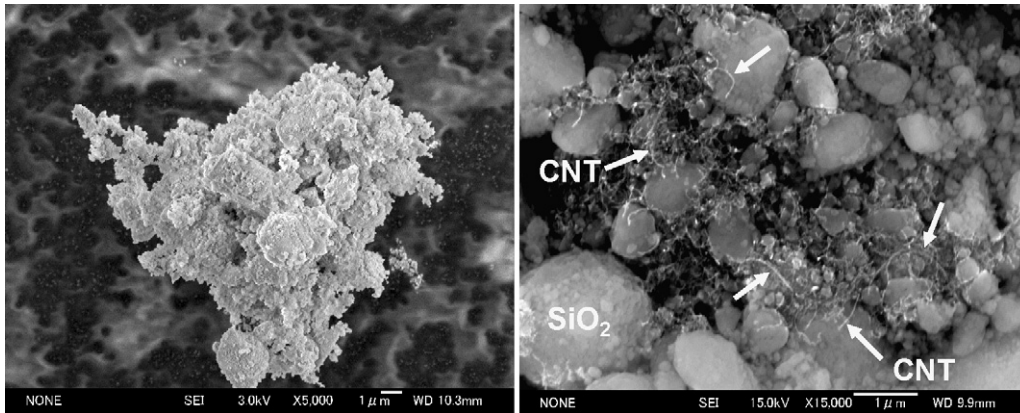


Fig. 1. Granulated amorphous silica particles with porous structure, including un-bundled carbon nanotubes inside (CNT-SiO₂ hybrid particles).

The structural evaluation by XRD analysis on the sintered magnesium composites is carried out when applying the sintering temperature of 823 K in the SPS process. This sintering temperature is enough to accelerate the reaction between magnesium and SiO₂ powders as mentioned above. Fig. 3 indicates the XRD patterns of the CNT-SiO₂ composite particles (a), the sintered pure magnesium (b), the sintered magnesium composites including CNT-SiO₂ particles of 5 mass% (c) and 10 mass% (d). In the case of (a), the broad profile with no crystalline peak is detected. This means that silica raw particles have completely amorphous structure. As shown in (b), Mg peaks are mainly detected in the profile, and a small one of MgO is also observed due to the original surface oxide films of raw magnesium powder. When using the elemental mixture of magnesium and SiO₂ powders coated with CNTs, both peaks of Mg₂Si and MgO are obviously detected in the profiles (c) and (d). Their intensities of the sintered material containing 10 mass% CNT-SiO₂ composite particles are extremely larger than those with the content of the composite particles with 5 mass%. This means that the content of Mg₂Si and MgO compounds via the solid-state synthesis increases during sintering at 823 K. Furthermore, when applying the annealing treatment at 1373 K in argon gas atmosphere to the material (d), no crystalline SiO₂ peak is detected by XRD analysis. In general, the crystallization temperature of the amorphous silica originated in rice husks is 1323 K or more [19], and the crystalline silica such as cristobalite or tridymite is detected in XRD analysis. Accordingly, no crystalline peak of SiO₂ detected in (d)

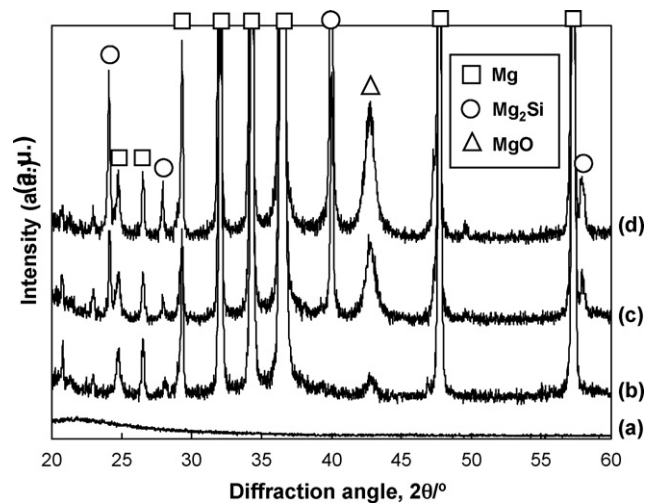


Fig. 3. XRD patterns of CNT-SiO₂ composite particles (a), sintered pure magnesium (b), sintered magnesium composites including CNT-SiO₂ particles of 5 mass% (c) and 10 mass% (d).

indicates that the amorphous silica raw particles have been completely reacted with the magnesium powders to form both Mg₂Si and MgO during SPS process at 823 K. Fig. 4 shows SEM-EDS analysis results of the sintered magnesium material including 10 mass% CNT-SiO₂ composite particles (a), compared to the P/M pure magnesium (b). As shown in Fig. 4(a), Si elements are detected at the primary particle boundaries (PPBs) of the magnesium matrix. This means that the synthesized Mg₂Si compounds exist at the PPBs, and nanotubes are also dispersed at the same boundaries. On the other hand, the sintered pure magnesium material with no nanotube reveals network-structure of magnesium oxides at the PPBs shown by arrows in Fig. 4(b). However, it indicates a good metallurgical bonding between magnesium powders without any defects and pores at the boundaries. Table 1 shows Rock-well hardness (scale F) measurements of the sintered magnesium composite reinforced with CNT and Mg₂Si. With increase in the reinforcement content,

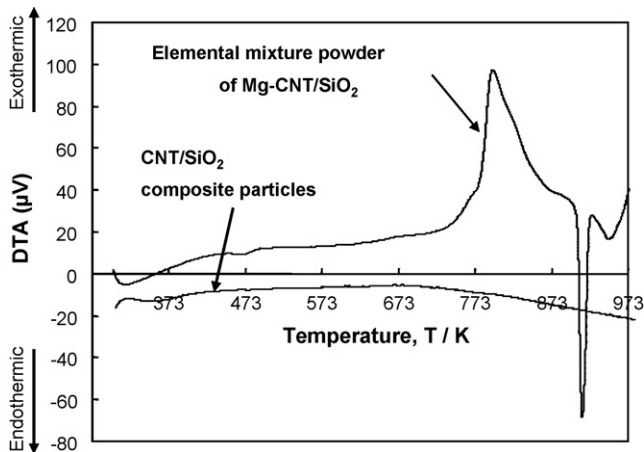


Fig. 2. DTA profiles of CNT-SiO₂ hybrid particles and elemental mixture of magnesium with hybrid particles (content; 10 mass%) in heating up to 973 K under argon gas supplement with 2.5 ml/s.

Table 1
Rock-well hardness (scale F) of sintered magnesium composite reinforced with CNT/SiO₂ particles.

	10%	5%	0%
Ave.	54.8	43.9	21.6
Max.	58.6	45.0	24.1
Min.	51.2	43.2	19.4

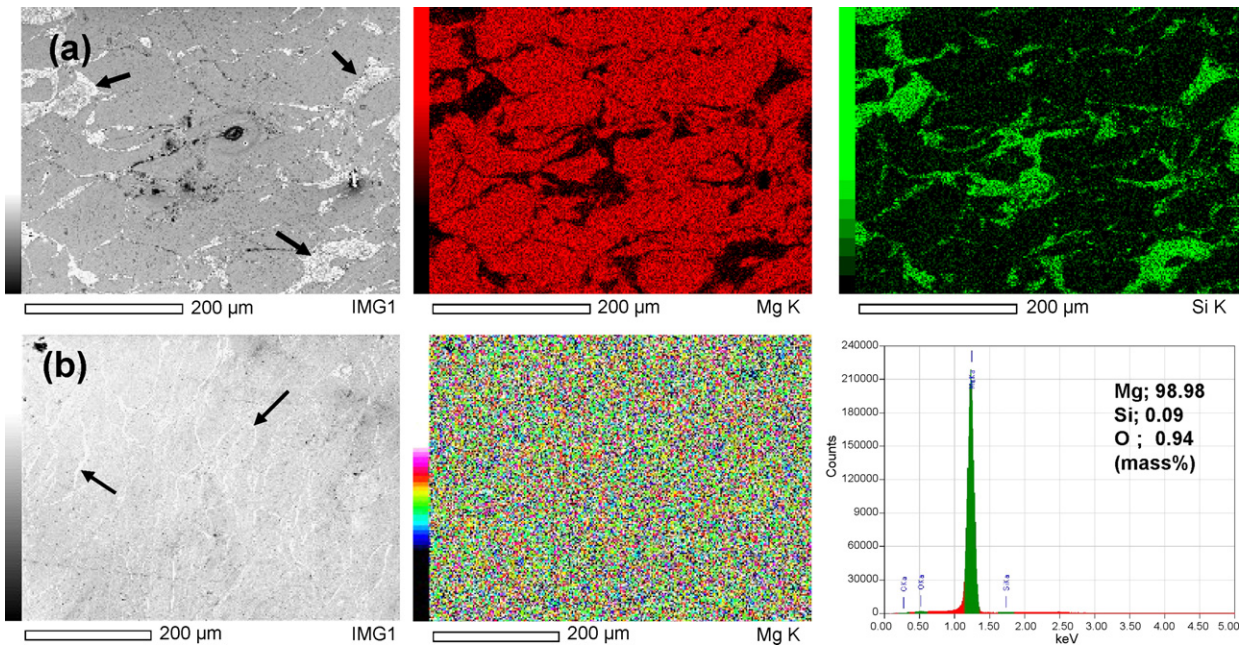


Fig. 4. SEM-EDS analysis results of sintered magnesium including 10 mass% CNT-SiO₂ hybrid particles (a) and pure magnesium (b).

the hardness gradually increases, and the composite with 10 mass% CNT-SiO₂ particles shows twice value as that of the pure magnesium with no reinforcement. When considering that each sintered material has a relative density of 98% or more, the increase of the hardness is due to the uniform distribution of Mg₂Si hard compounds [16] and un-bundled nanotubes in the matrix.

3.2. Tribological properties

Fig. 5 shows the changes of the friction coefficient (μ) of the sintered magnesium materials including CNT-SiO₂ composite particles of 10 mass% (a) and 5 mass% (b), compared to the pure magnesium with 0 mass% composite particles (c), when employing a SUS304 stainless steel ball as the counter material in the dry wear test. In the case of (a), the friction coefficient is the most stable, and its mean value (μ_0) is lowest of all specimens. The μ_0 value and its instability gradually increases with decrease in the content of the additive CNT-SiO₂ composite particles as shown in Fig. 5(b) and (c). The above results mean that the tribological behavior becomes stable by the uniform distribution of the additive reinforcements of CNTs and Mg₂Si contained in the sintered magnesium material. Fig. 6 shows the damaged area of the sliding surface of each sintered magnesium disc specimen after wear test observed by optical microscope. When containing the reinforcement of 10 mass% CNT-SiO₂ composite particles (a), a slightly abrasive wear, but no adhesion is observed on the sliding surface. The black area corresponds to both Mg₂Si compounds and CNTs. In the case of (b), the main damages are due to the abrasive wear attacked by the counter material, but some plastically deformed areas are also detected. The sintered pure magnesium with no additive (c) reveals both severe abrasive wear and adhesion at the sliding surface. The macro-observation on the surface also shows the stripe pattern damages vertical to the sliding direction. This is caused by a “stick-slip” phenomenon due to the repetition of the adhesion and detachment of the magnesium on the counter material under the dry sliding condition [24]. As a result, the friction coefficient change shows a typical behavior with a sharp fluctuation corresponding to a “stick-slip” phenomenon shown in Fig. 5(c). Fig. 7 indicates the SEM-EDS analysis result on the PPB, where the synthesized Mg₂Si

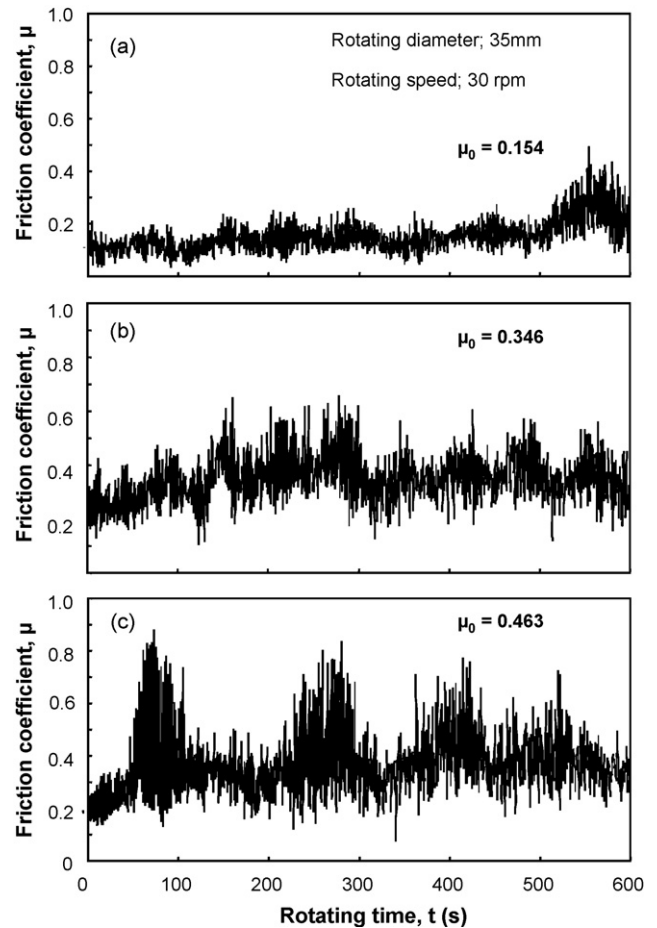


Fig. 5. Changes of the friction coefficient (μ) of sintered magnesium materials including CNT-SiO₂ composite particles of 10 mass% (a), 5 mass% (b) and 0 mass% (c), which are used as disc specimen, when employing a SUS304 stainless steel ball as counter material in the dry wear test.

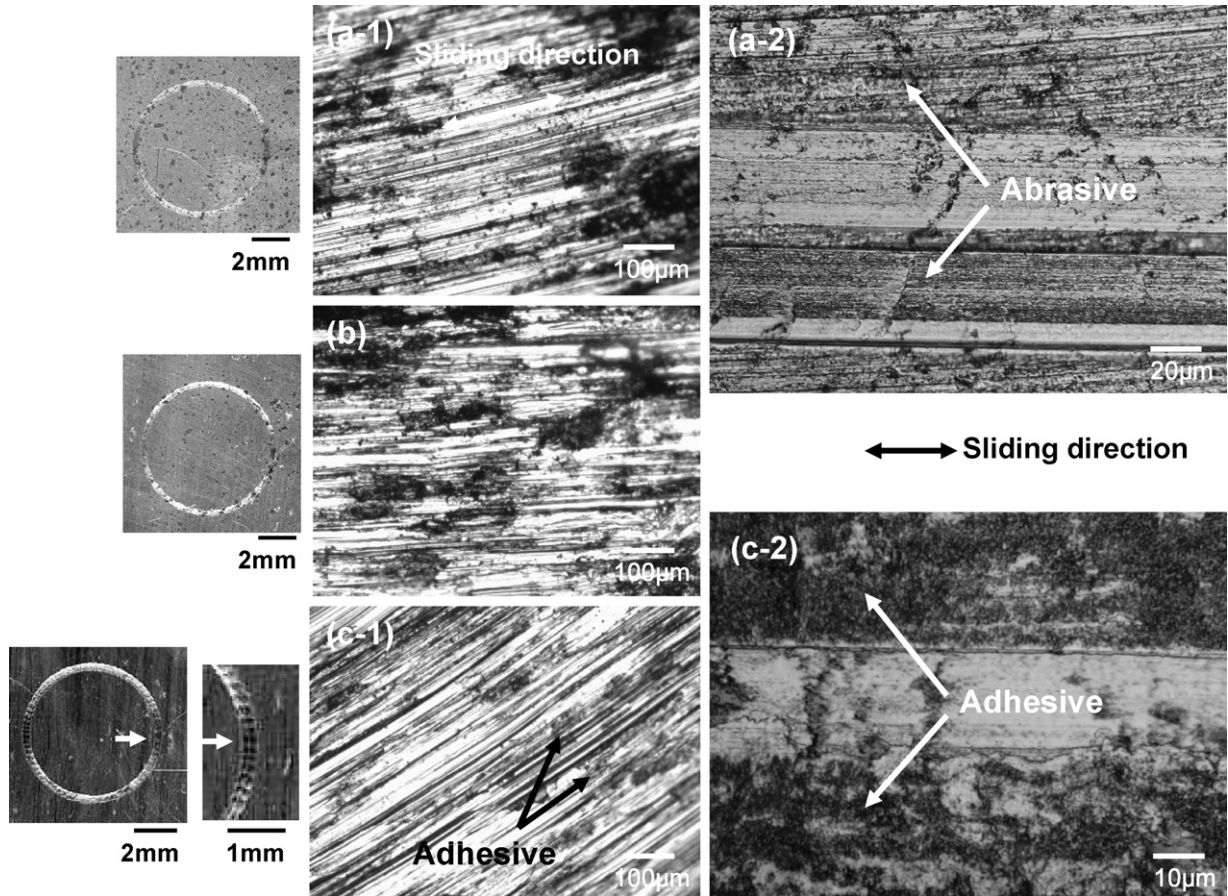


Fig. 6. Damaged area of sliding surface of each sintered magnesium disc specimen after wear test observed by optical microscope: CNT-SiO₂ hybrid reinforcement of 10 mass% (a), 5 mass% (b) and 0 mass% (c).

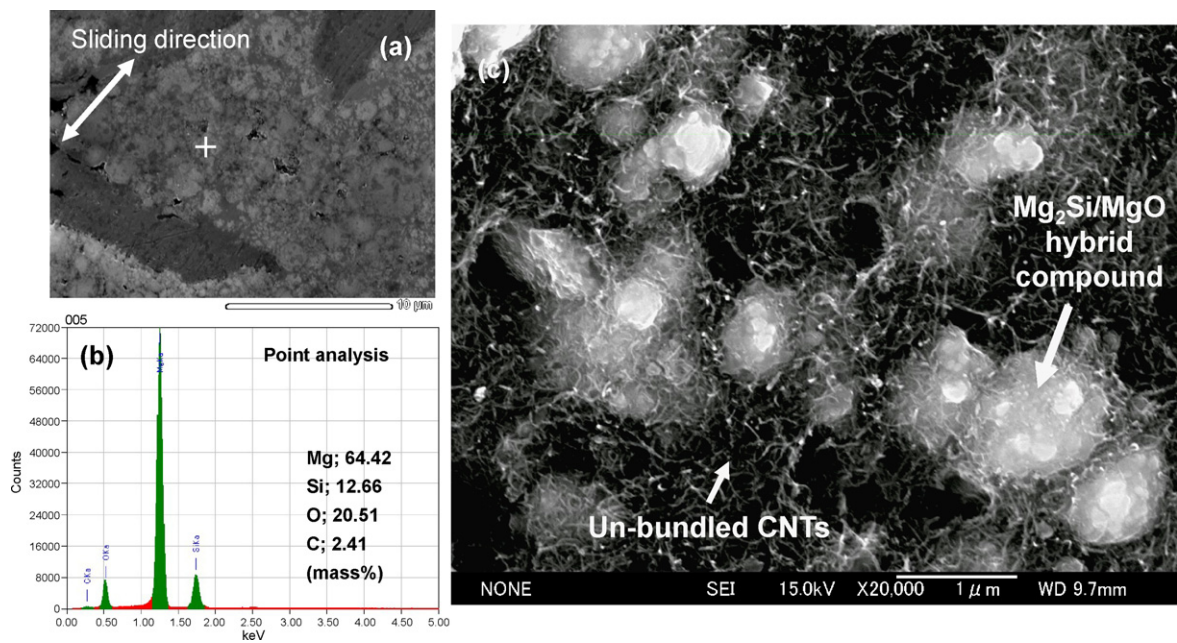


Fig. 7. SEM-EDS analysis result on primary particle boundaries, where synthesized Mg₂Si and MgO compounds exist, of sliding surface of sintered magnesium composite with reinforcement of 10 mass% after wear test.

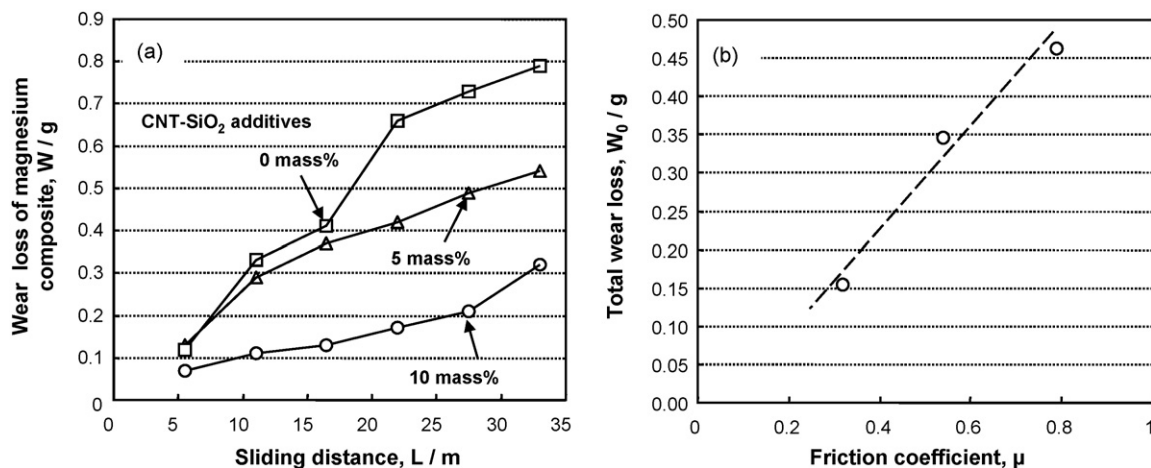


Fig. 8. Dependence of wear loss of magnesium composites on sliding distance (a), and relationship between total wear loss and mean friction coefficient (b).

and MgO compounds exist, of the sliding surface of the sintered magnesium composite including 10 mass% CNT-SiO₂ particles. In the magnified area of the reinforcement of Fig. 7(b), it consists of the white particles, corresponding to Mg₂Si and MgO hybrid compounds, and un-bundled nanotubes. There is no detached Mg₂Si and MgO compound from the sliding surface because of a strong bonding between the magnesium matrix and their compounds via the solid-state synthesis as mentioned above. In particular, the network-structured CNTs are formed around the synthesized composite particles, and the individual CNT covers the sliding surface. Accordingly, the reason why the sintered magnesium composite material with CNTs and Mg₂Si/MgO particles showed a superior tribological behavior with a low and stable friction coefficient is due to both improved defensive by the synthesized Mg₂Si hard particles [17] and the self-lubricant and bearing effects of the network-structured nanotubes dispersed in the matrix. Fig. 8 summarizes the tribological properties of the sintered magnesium composite reinforced with un-bundled CNTs and Mg₂Si/MgO compounds under dry conditions. Fig. 8(a) shows a change of the wear loss of the magnesium composite specimen as a function of the sliding distance. All specimens indicate that the wear loss gradually increases with increase in the distance. However, the wear rate depends on the content of CNT-SiO₂ additives. In the case of 10 mass% CNT-SiO₂ particles, the wear rate is constant through the wear test, and tribological behavior is stable. When the content of the additives is 5 mass%, it drastically increases at the initial stage of the wear test until 200 s after starting the test. By considering the friction coefficient changes shown in Fig. 5(b), the lubrication effect of CNTs on the sliding conditions is not stable, and causes the large wear loss. After that, the magnesium composite shows a lower wear rate. As shown in Fig. 8(b), the total wear loss is proportional to the friction coefficient. It means that both of the uniform distribution of Mg₂Si hard particles and the lubricant effect of un-bundled CNTs are effective to improve the tribological properties of the sintered magnesium composite by decreasing the friction coefficient and wear loss during sliding.

4. Conclusion

The sintered magnesium composite material reinforced with the carbon nanotubes and Mg₂Si/MgO compounds has been developed by powder metallurgy process when using the elemental mixture of pure magnesium powders and amorphous porous sil-

ica particles containing CNTs as a starting material. During sintering the mixture powder, the solid-state synthesis of Mg₂Si and MgO via the deoxidation and oxidation reaction occurred. The tribological properties of the sintered magnesium material were significantly improved by the additive reinforcement, and the friction coefficient was low and stable under the dry sliding condition. Hard Mg₂Si intermetallic compounds distributed in the matrix of the composite were effective for improving the wear resistance in contacting a SUS304 stainless steel ball. Nanotubes had an important role to form the lubricant condition at the sliding interface between the sintered magnesium and the counter material due to their network structure on the sliding surface.

References

- [1] Weijiu Huang, Bin Hou, Youxia Pang, Zhongrong Zhou, *Wear* 260 (2006) 1173–1178.
- [2] J. An, R.G. Li, Y. Lu, C.M. Chen, Y. Xu, X. Chen, L.M. Wang, *Wear* 265 (2008) 97–104.
- [3] Naing Naing Aung, Wei Zhou, Lennie E.N. Lim, *Wear* 265 (2008) 780–786.
- [4] C.Y.H. Lim, D.K. Leo, J.J.S. Ang, M. Gupta, *Wear* 259 (2005) 620–625.
- [5] S.C. Sharma, B. Anand, M. Krishna, *Wear* 241 (2000) 33–40.
- [6] Q.B. Nguyen, M. Gupta, *Compos. Sci. Technol.* 68 (2008) 2185–2192.
- [7] X.J. Wang, X.S. Hu, K. Wu, K.K. Deng, W.M. Gan, C.Y. Wang, M.Y. Zheng, *Mater. Sci. Eng.: A* 492 (2008) 481–485.
- [8] X.H. Men, Z.Z. Zhang, H.J. Song, K. Wang, W. Jiang, *Compos. Sci. Technol.* 68 (2008) 1042–1049.
- [9] L.C. Zhang, I. Zarudi, K.Q. Xiao, *Wear* 261 (2006) 806–811.
- [10] S.M. Zhou, X.B. Zhang, Z.P. Ding, C.Y. Min, G.L. Xu, W.M. Zhu, *Composites: Part A* 38 (2007) 301–306.
- [11] K.T. Kim, S.I. Cha, S.H. Hong, *Mater. Sci. Eng. A* 449–451 (2007) 46–50.
- [12] W.X. Chena, J.P. Tub, L.Y. Wangb, H.Y. Gana, Z.D. Xua, X.B. Zhangb, *Carbon* 41 (2003) 215–222.
- [13] L.Y. Wang, J.P. Tu, W.X. Chen, Y.C. Wang, X.K. Liu, Charls Olk, D.H. Chengd, X.B. Zhang, *Wear* 254 (2003) 1289–1293.
- [14] M. Damjanovic, T. Vukovic, I. Milosevic, *Euro. J. Phys. B* 25 (2002) 131–134.
- [15] H.W. Kroto, J.R. Heath, S.C. O'Brien, R.F. Curl, R.E. Smalley, *Nature* 318 (1985) 162–163.
- [16] L.F. Mondolfo, *Aluminum Alloys: Structure and Properties*, Butterworths, London, 1976, p. 566.
- [17] K. Kondoh, H. Oginuma, A. Kimura, S. Matsukawa, T. Aizawa, *Mater. Trans.* 44 (2003) 981–985.
- [18] K. Kondoh, H. Oginuma, T. Aizawa, *Mater. Trans.* 44 (2003) 524–530.
- [19] J. Umeda, K. Kondoh, Y. Michiura, *Mater. Trans.* 48 (2007) 3095–3100.
- [20] J. Umeda, K. Kondoh, Y. Michiura, *Trans. Joining Weld. Res. Inst.* 36 (2007) 17–21.
- [21] K. Kondoh, H. Oginuma, J. Umeda, T. Umeda, *Mater. Trans.* 46 (2005) 2586–2591.
- [22] M.F. de Souza, P.S. Batista, I. Regiani, J.B.L. Liborio, D.P.F. de Souza, *Mater. Res.* 3 (2000) 25–30.
- [23] B. Fugetsu, W. Han, N. Endo, Y. Kamiya, T. Okuhara, *Chem. Lett.* 34 (2005) 1218–1219.
- [24] R. Smith, D. Mulliah, S.D. Kenny, E. McGee, A. Richter, M. Gruner, *Wear* 259 (2000) 459–466.